	ATLAS Inner Detector
	Concept of Radiation Monitor

ATLAS Project Document No:	*Institute Document No.*	*Created: 06/09/04*	*Page:* **1 of 22**
		Modified: **10/4/2006 10:00:00 AM**	*Rev. No.:* **A**

Design and Functional Specification of ATLAS Radiation Monitor

This document outlines the design and expected functionality of the Radiation Monitor (RM). The RM builds together with Beam Conditioning Monitor (BCM) the ATLAS Radiation Monitoring System.

Prepared by:	*Checked by:*	*Approved by:*
Gregor Kramberger, J. Stefan Institute **Vladimir Cindro, J. Stefan Institute** **Irena Dolenc, J. Stefan Institute** **Igor Mandic, J. Stefan Institute** **Marko Mikuž, J. Stefan Institute**		

Distribution List

History of Changes

Rev. No.	Date	Pages	Description of changes
	06/09/04		V 1.0
	02/03/05		V 1.1
	13/11/05		V 1.2
	06/08/06		V 2.0

0 Introduction

This document outlines the conceptual design considerations and expected functionality of the Radiation Monitor (RM) which is the part of the ATLAS Radiation Monitoring System (ARMS). Its goals are

- Measurement of the **t**otal **i**onising **d**ose (**TID**) at various locations in the detector
- Measurement of non-ionising energy loss (NIEL) at various locations in the detector.
- Measurement of the degradation of DMILL bipolar transistors performance in the Inner Detector.

The measurements of TID and NIEL are vital for understanding the changes in performance during the operation of the ATLAS detector, verifying simulations and thus giving a chance to plan a better operation scenario.

It is foreseen that radiation doses will be measured with sensors which can be read out online in the whole ATLAS. The basic unit will be a RM sensor board (RMSB) which will host radiation detectors connected to the readout cables.

In the Inner Detector RMSB will be placed at 14 locations (see section 6) and will provide on-line information of ionization dose in SiO_2, NIEL in silicon and damage to the DMILL transistors. Because of large range of doses, very limited access, and relatively low number of locations due to limited space, RMSB in the Inner Detector will host a number of radiation detectors which will cover the large range of doses and provide a high level of redundancy.

Outside Inner detector the range of expected dose levels is smaller therefore TID and NIEL damage will be measured with simplified version of RMSBs containing only two sensors, one for each type of radiation damage (TID and NIEL). There are presently 50 locations foreseen for RMSBs: 24 in calorimeter (6 in TILE and 18 in LAr), 10 for electronics at PP2, 16 in Muon EC.

1 Sensors

1.1 DOSE measurement

1.1.1 RADFETS

The on-line measurement of the **T**otal **I**onising **D**ose (TID) is nowadays most commonly [1,2,3] performed with **Rad**iation **F**ield **E**ffect **T**ransistors (RADFET).

The measurement technique exploits the change of the threshold voltage (voltage needed at the gate of the transistor to achieve conduction) due to irradiation in p-MOS transistors. The radiation induced electrons and holes have different mobilities in the oxide and while electrons are collected by the gate electrode the holes are trapped in the oxide or at the oxide-silicon surface. Consequent change in electric field must be compensated by a larger negative gate voltage V_G needed to open the channel. Therefore, the increase of the gate voltage at fixed drain current is the measure of the received dose. The crucial parameter of the RADFET is the oxide thickness as it determines the sensitivity and dynamic range. RADFETs with thin oxide (~100 nm) are suitable for measurements of larger doses, however with smaller sensitivity, while thicker oxide allows higher sensitivity at smaller dynamic range as the increase of V_G becomes the limiting parameter.

A RADFET has 3 connections (gate, source, drain). In the most usual configuration gate and drain are common, so a RADFET can be read-out using 2 contacts. The read-out is done by applying constant current between the two contacts and measuring the voltage drop. The typical currents are in the range of few hundred µA. The actual value of current is chosen in such a way that the voltage drop is least dependent on temperature. Typical voltage drops for the Mrad-RADFETs are below 30 V with typical break-down voltages of around 70 V. The voltage drop changes with time after setting the bias, therefore it is important to use the same read-out cycle (apply I, measure V few seconds later) as during calibration. Response curves of RADFETs with different sensitivity can be seen in Figs 1,2.
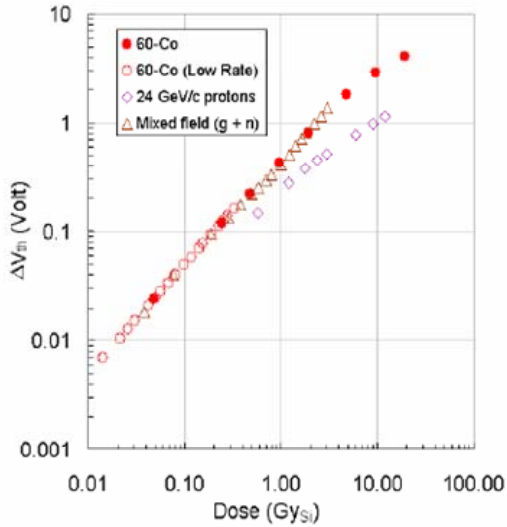
Figure 1: Voltage shift vs. dose curve for high sensitivity (1.6 μm thick oxide) RADFET (from [3]) after irradiation with different particles.
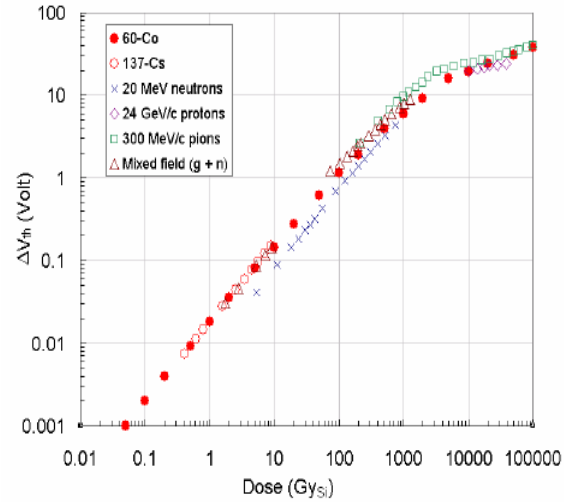
Figure 2: Voltage vs. dose of a low sensitivity RADFET (0.25 μm oxide thickness) after irradiation with different particles.

The group of CERN TS-LEA department has chosen the RadFETs which will be used for radiation monitors in LHC experiments. High sensitivity sensors will be RadFETs with 1.6 μm oxide thickness produced by CNRS LAAS, Toulouse, France. Thin oxide radfets from REM Oxford Ltd. UK with two different oxide thicknesses will be used in the inner detector only: 0.25 μm and 0.13 μm in order to cover the expected dose range with the maximum available bias voltage (28 V). More details about properties of chosen device types can be found in Ref. [3].

RadFETs will be packaged in the LD36 ceramic chip carrier. Detailed layout and connectivity can be found in section 6.3 at the end of this report or at (http://lhc-expt-radmon.web.cern.ch/lhc-expt-radmon/solid_state_group/36LDCC-layout.pdf)

1.2   Bulk damage (NIEL) measurement

1.2.1   *Leakage current measurements of pad-detectors (diodes)*

The bulk damage in silicon has been studied in great detail by ROSE (RD48) collaboration [4]. The leakage current increase (ΔI) after irradiation has been found to be directly proportional to **N**on-**I**onising **E**nergy **L**oss (NIEL) and independent on the material type (same for diffusion oxygenated and standard float zone sensors, Chochralsky and epitaxial Si sensors). The 1 MeV neutron equivalent fluence (Φ_{eq}) is determined from $\frac{\Delta I}{\alpha(t,T) \cdot V} = \phi_{eq}$, where $\alpha(t,T)$ is the leakage current damage constant and V the sensitive volume of the detector. An important fact is also that the annealing of the leakage current (change of α with time after irradiation) at different temperatures is well known.

A silicon pad detector-diode with a guard ring structure (0.5 x 0.5 cm^2) will be used to measure the leakage current increase. In order to have detectors fully depleted already at voltages below 30 V a very thin detectors will be used: 25 μm thick detectors processed on epitaxial silicon of 50 Ωcm are foreseen [5]. These detectors invert at $\Phi>10^{15}$ cm^{-2}, which ensures full depletion during the lifetime of the experiment. The leakage current anneals with time, a strongly temperature dependent process. Most of the experimental studies have been so far done at $>20^{\circ}$C . Therefore controlled resistive heater will be put on the RMSB which will maintain constant temperature ($\sim 20\,^{\circ}$C) of the sensor board.

To prove the principle we irradiated four 25 μm Epi-Si samples with reactor neutrons to three different equivalent fluences: 2×10^{13} cm^{-2}, 10^{14} cm^{-2} and 2×10^{14} cm^{-2}. After irradiation the diodes were stored for about a month at -17°C. An example of a current-voltage characteristic (I-V) and a capacitance-voltage characteristic (C-V) is shown in Figs. 3,4 (**note** no annealing at elevated temperature was performed before these measurements) . The measurements were performed in a probe-station.
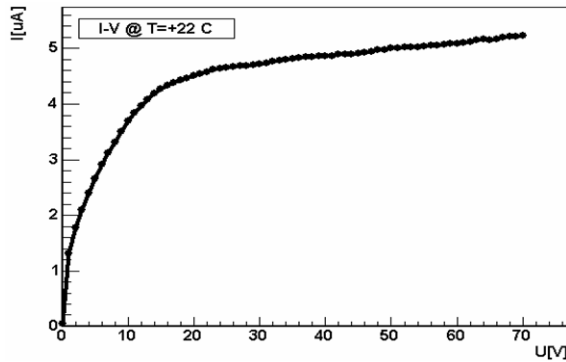
Figure 3: Reverse current dependence on voltage for 25 μm epi-Si diode irradiated to equivalent fluence of 10^{14} cm^{-2} with reactor neutrons.
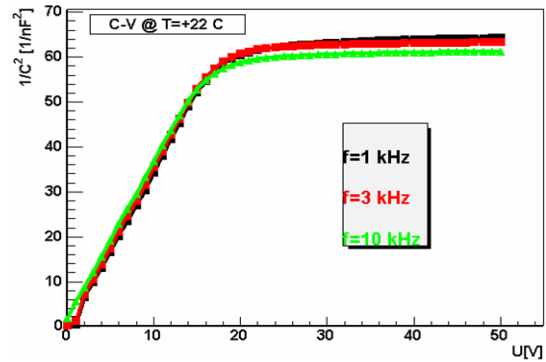
Figure 4:C-V characteristics of the same diode as shown in Fig. 3 at different frequencies.

The dependence of full depletion voltage and leakage current (normalized to 20°C) on fluence is shown in Figs. 5,6. It is clear that 28 V will be sufficient to fully deplete the detector over the entire period of operation. As the leakage current decreases by roughly factor of 2 when temperature is reduced by 7°C it is clear that measurements at higher temperatures yield larger sensitivity. This is particularly important for running at low luminosity where only approximately 1.5% of the final fluence will be received per year. Annealing studies on these samples are shown in Figs. 7,8.
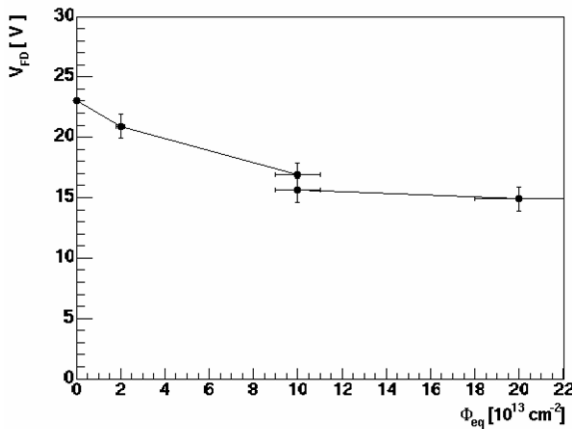

Figure 5: Full depletion voltage before the end of initial annealing phase as a function of equivalent fluence.
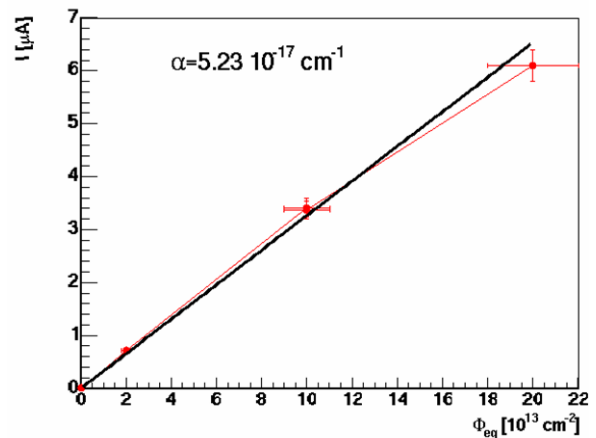
Figure 6: Leakage current normalized to 20°C (right) as a function of equivalent fluence before completion of beneficial annealing.
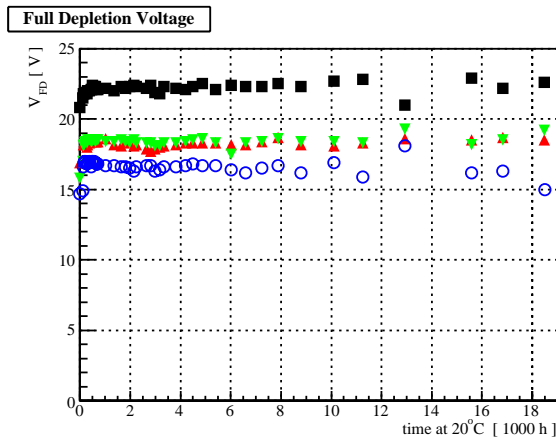
Figure 7: Annealing of FDV at 20°C for diodes irradiated to fluences 2e13, 1e14 (two diodes) and 2e14 n/cm²
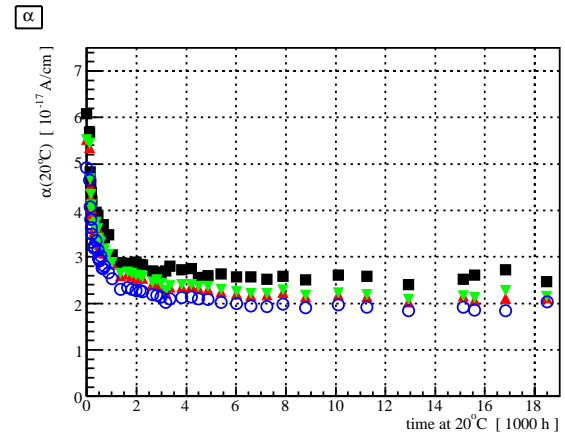
Figure 8: Annealing of leakage current factor α at 20°C for diodes irradiated to different fluences.

1.2.2 *Measurement of forward bias in PIN diodes*

The voltage drop on the intrinsic base of PIN diodes, when operated in forward bias, depends on the minority carrier lifetime. As a consequence of bulk damage, minority carrier lifetime is decreased which increases voltage drop on the intrinsic base. Measurement of forward bias at given forward current can be used to measure bulk damage in silicon [6]. Sensitivity to radiation increases with the width of intrinsic base.

Commercial pin diodes (OSRAM – BPW34F) operated under forward bias [7,8] will be used to measure NIEL equivalent bulk damage in the inner detector. The measure of bulk damage is forward bias at 1 mA of forward current. These diodes can be used to measure fluences larger than 4×10^{12} n/cm² because forward bias until this fluence is reached doesn't change or is even slightly falling with increasing fluence. The diodes can be made sensitive to lower fluences by pre-irradiating them with neutrons to about 4×10^{12} n/cm² [3] and so skip the no-sensitivity part of the characteristics. OSRAM diodes which will be mounted on Inner Detector RMSBs were preirradiated with neutrons in reactor in Ljubljana to 3×10^{12} n/cm². In this way, some information about low fluence will be obtained also from them, without loosing any functionality for measurements of high fluences.

Lower fluences, relevant outside of the Inner detector as well as during the low luminosity years in the Inner detector, will be measured by more sensitive (longer base) silicon PIN diodes provided by CMRP, Wollongong Australia [9]. These diodes will be used for measurements of bulk damage for fluences in the range between few times 10^{10} n/cm² to few times 10^{12} n/cm².

Several BPW-34F diodes and one CMRP diode were irradiated with neutrons in the TRIGA reactor in Ljubljana. Increase of forward voltage at 1 mA forward current as a function of reactor neutron fluence expressed in 1 MeV neutrons NIEL equivalent in Si is shown in Figs. 9,10. More details about these devices can be found in Ref. [3].
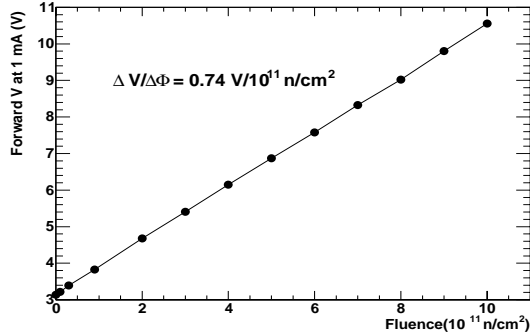
Figure 9: Forwad voltage vs. 1 MeV neutron fluence immediately after irradiation for high sensitivity diode (CMRP).
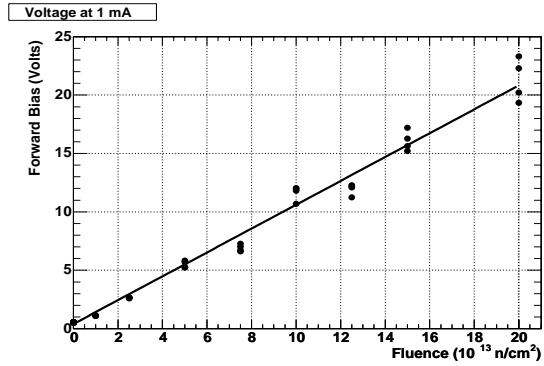

Figure 10: Forwad voltage vs. 1 MeV neutron fluence immediately after irradiation for low sensitivity diode (BPW-34F).

Forward voltage after irradiation anneals with time if diodes are kept at 20°C, which is the planed operating temperature of RMSBs in ATLAS. Annealing studies at different temperatures are underway and some preliminary results are shown in Figs. 11,12.
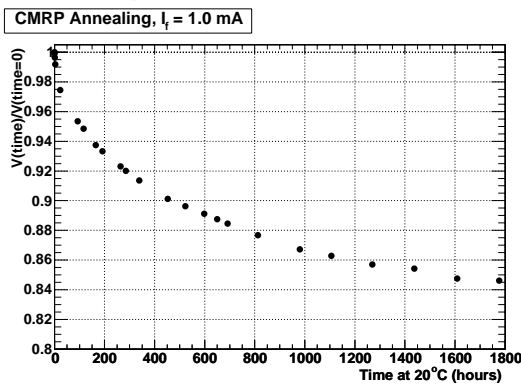

Figure 11: Annealing of forward voltage at 1 mA forward current with time after irradiation for high sensitivity diode irradiate to 10^{12} n/cm^2
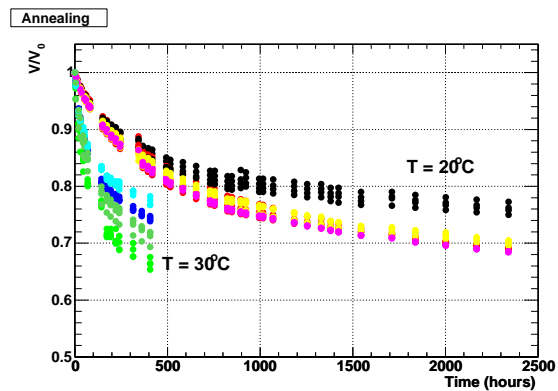

Figure 12: Annealing of forward voltage at 1 mA forward current with time after irradiation for several BPW-34F diodes irradiated to different fluences ranging from 10^{13} n/cm^2 to $2x10^{14}$ n/cm^2

1.3   DMILL test structures measurements

DMILL bipolar transistors are used in SCT and TRT front-end electronics. Bipolar transistors are sensitive to both, bulk and ionisation damage, which cause degradation of common emitter current gain factor $\beta=I_c/I_b$ (collector current/base current). The reduction of β is the main cause for degradation of performance (smaller gain, larger noise) of bipolar front-end electronics used in the Inner Detector. It is therefore important to have information about the condition of DMILL transistors, to understand the performance of readout electronics. In addition, it is a feature of DMILL transistors, that their β is very sensitive also to thermal neutrons [10].

Thermal neutrons contribute only very little to NIEL in pure silicon. But they can cause serious damage to bipolar transistors with boron-doped base. The He and Li ions from reaction B+ thermal-n-> Li + He + γ, can cause substantial bulk damage within their small range (5 μm). This reaction is important because of its large cross section. In [10] it was shown that DMILL bipolar transistors are very sensitive to this kind of damage. It was shown also that the damage caused by fast hadrons and thermal neutrons is additive. From measurement of change of common emitter current gain (i.e. base current increase at given

collector current) in DMILL transistors the fluence of thermal neutrons can be measured, if NIEL equivalent fluence is known, because:

$$\frac{\Delta I_b}{I_c} = k_{eq} \cdot \Phi_{eq} + k_{th} \cdot \Phi_{th},$$

where k_{eq} and k_{th} are equivalent and thermal neutron damage factors, respectively. Damage factors are measured in calibration irradiations as shown in Fig. 13.
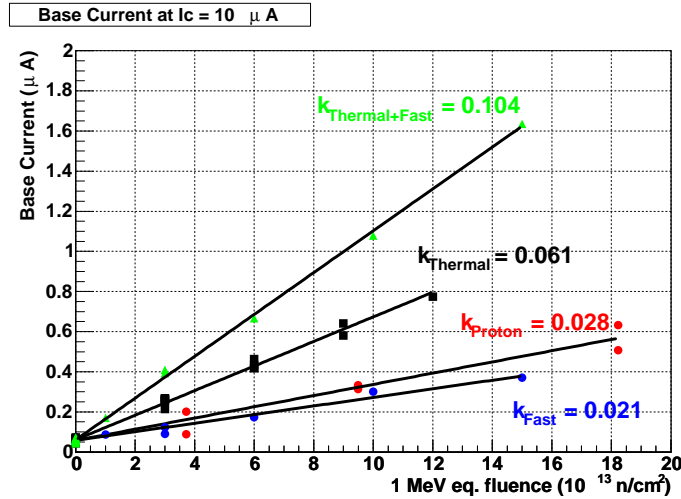

Figure 13: Base current at 10 µA collector current (proportional to 1/β) as a function of fluence. For protons, fast neutrons and for mixture (thermal+fast, $\Phi_f/\Phi_{th} \sim 0.7$) fluence is in 1 MeV equivalent neutrons. For thermal neutrons x-axis means the fluence of thermal neutrons.

It is therefore essential to monitor thermal neutron fluence or to use DMILL test structures (transistors) to get the most reliable estimate on damage inflicted to SCT and TRT front-end electronics. The latter can be used also to estimate fluence of thermal neutrons in the Inner Detector.

DMILL test structures will be mounted on the RMSB to monitor the degradation of $\beta = I_c/I_b$ (collector current/base current) parameter.

2   RSMB hybrid

Inner detector RMSB will host 3 radfets (three oxide thicknesses: 1.6, 0.25 and 0.13 μm), CMRP diode, BPW-34 diode, epi-Si diode and 2 DMILL test structures. The temperature sensor will be 10 kOhm NTC sensor.

An aluminium oxide (Al_2O_3) hybrid will ensure mechanical support and temperature stability for the sensors of the ID-RMSB. Its good heat conductivity and high electrical resistance make it an appropriate candidate. Conductive lines of few hundred microns on both sides of ~600 μm thick substrate can be made as well as gold plating to ensure a wire-bondable contacts. Heater will be made by deposition of resistive paste (300 Ohm) on one side of the hybrid while sensors will be mounted on the other. The heater will be used to stabilize the temperature of the RMSB few degrees above (maximum expected) ambient temperature.

Layout of the ID-RMSB can be seen in Figs. 14,15. The contacts on the ceramics will be soldered to a PCB frame with thin wires. The twisted-pair cables soldered to the PCB will be used for connection to the read-out electronics. The PCB frame with hybrid will be placed in a housing made from PEEK plastic which will mechanically protect the sensors and provide an air-gap for thermal insulation.

At locations outside ID, RMSBs won't be thermally stabilized and heat conductive ceramics will be replaced by PCB. The two radiation sensors (CMRP PIN diode and RadFET) will be mounted on it. The photographs of the populated ID-RMSB and ATLAS-RMSB (for locations outside of the ID) are shown in Figs. 16 and 17. An aluminium housing for the ATLAS-RMSB will be made to mechanically protect the sensors on the board. Drawings of boards and boxes with dimensions can be found in section 6.
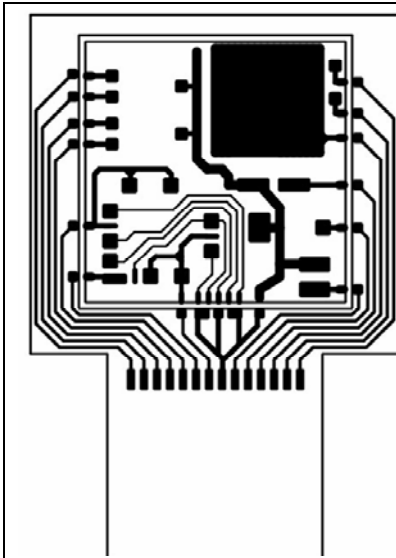

Figure 14: The mask of the prototype hybrid for ID-RMSB and PCB support frame. The top side of ceramic hybrid and PCB support frame is shown with sensor pads and signal lines
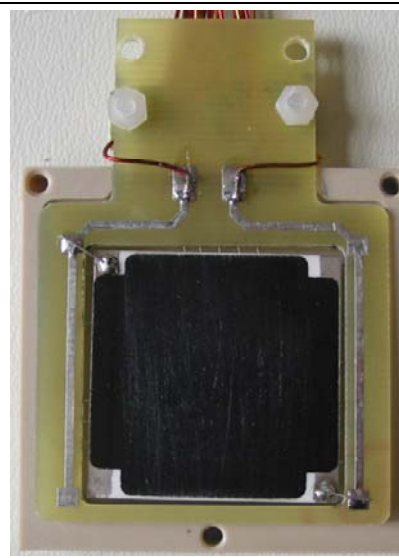

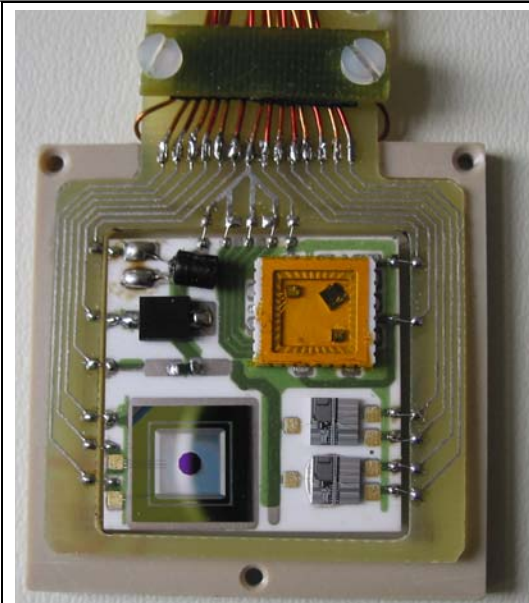*Figure 15: . The photograph of the bottom side of the hybrid in housing. The black pad is resitive paste.*

Figure 16: Populatedhybrid of an ID RMSB connected to a PCB frame in the bottom part of PEEK housing (Epi-Si bottom left, DMILL transistors bottom right, PIN diodes (top left and RadFETs top right).Outer dimension of the plastic housing box is 4cm x 4cm
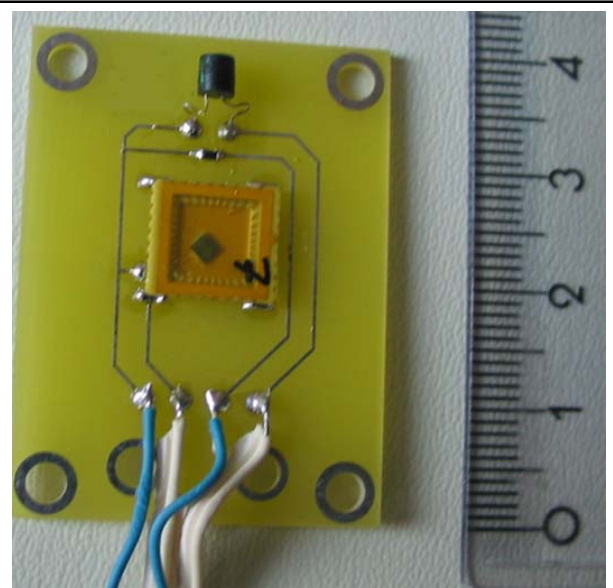

Figure 17: Populated ATLAS RMSB (High sensitive pin diode top, NTC middle and RadFET package bottom).

3   RMSB Read-out

The general requirement for the radiation monitoring read-out is that it should use standard ATLAS Detector Control System (DCS) read-out boards ELMB [11,12] and ELMB-DAC [13]. This saves enormous effort in building a dedicated read-out system and ensures full compatibility, spare parts availability and easy integration into the ATLAS DCS system. On the other hand this reduces to some extent the flexibility of the RMSB.

The readout of the RMSB is based on ELMB, which communicates over the CAN bus with PC running SCADA software (PVSSII) and communicates to ATLAS DCS. Each ELMB hosts 64 12-bit ADC channels (0-4.5 V) with the conversion frequency ranging from 2-100 Hz. Up to four 16 channel 12-bit DAC boards can be connected to and controlled by the ELMB.

The output from ELMB-DAC [13] is current, which can be converted, if needed, to voltage via a resistor. External power supply with max. voltage of 30 V can be connected to DAC boards. The maximal output current of each DAC channel can be set between 1 and 20 mA by choosing appropriate value of one onboard resistor operated per channel. Maximum output voltage of a DAC channel is set by the supply voltage (i.e. 30 V). However, care must be taken about the power dissipation on some of the FETs on DAC board so current can not exceed certain limits at given voltage (see Ref. [13] for more details).

Only DAC boards used to readout ID RMSBs will use external power of 30V, while outside ID the power will be taken from the CAN bus (VDP line) which is in the range 10-15 V. This is sufficient to operate sensors over entire lifetime of ATLAS.

3.1.1   Details about readout of radiation sensors

- EPI-Si diodes: diode will be connected to DAC in parallel with 40 kΩ resistor to bias the diode during readout. Bulk and guard ring will be connected to ground via 100 kΩ resistors. Voltage on these resistors will be measured by ADC to estimate bulk and guard-ring currents. Care must be

taken to select the value of measurement resistor so that voltage drop on them, caused by leakage current, does not push bias voltage below FDV.

- PIN diodes: a current pulse <= 1mA will be injected and voltage drop measured between the contacts of the DAC. The range of the ADC is ~5 V maximum, therefore a differential attenuator will be used. The attenuator circuit will be on the patch panel board (see Figs 23, 25, 26). To reduce the input impedance of the ADC channel (hence the noise) capacitors will be used along with the resistors. A choice of very high resistor (high resistance of the voltmeter) is governed by the fact that ground loop currents must be small in order not to disturb the measurement.

- RADFETs: readout is similar to the readout of the PIN diodes with somewhat smaller current injected (100 μA LAAS, 160 μA REM radfets). Same differential attenuators as for the PIN diodes will be used.

- DMILL structures: Degradation of $\beta = I_c/I_b$ will be measured. The base current must be measured at given collector current. As the $I_b << I_c$ a single DAC can be used in the circuit which is a part of PP2 circuit shown in Fig. 23. There is circuitry on PP2 boards which protects DMILL transistors from over voltage and ESD discharges. The values of resistors should be chosen to meet the ADC range.

- 10 kOhm NTC temperature sensor (103KT2125T) will be used. Sensor will be connected to the output of 2.5 V reference voltage on ELMB in series with a 100 kOhm resistor. Voltage on the sensor will be measured to estimate the resistance of the sensor and therefore its temperature.

- Heater: to ensure constant and controlled temperature of the RMSB resistive heaters will be processed directly on the backside of the hybrid. Power will be provided to the heater using 4 DAC output channels. Maximum current output of 4 channels together is 80 mA at 30 V, providing sufficient power to maintain a temperature difference of ~40°C.

4   First tests

In Fig 18. results of tests of sensitivity of the system is shown. Full readout chain: computer - CAN bus – ELMB – DAC – RMSB, with 14 m long cables has been set up and sensors were read out every 10 minutes. For these measurements temperature stabilization was not used. During the measurement temperature varied in the range from 18.8 to 23.6 °C. Temperature corrections were done from measured correlation between readout voltage and temperature on the RMSB. The MRSB was wsposed to radiation from [22]Na source for about 80 hours to estimate the sensitivity of RADFETs.
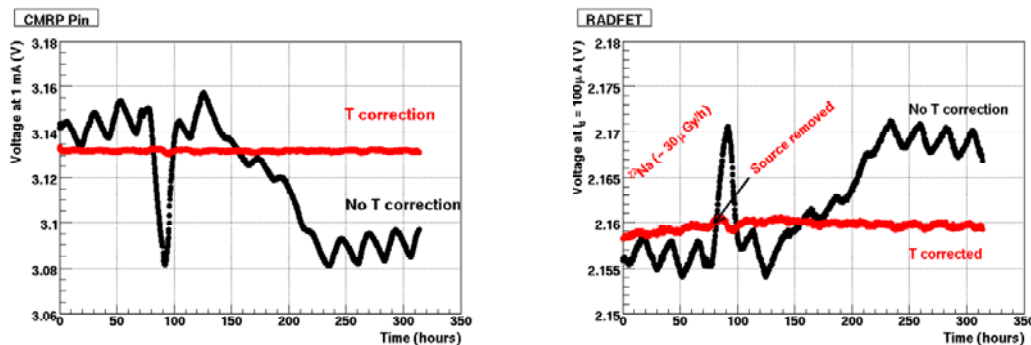

Fig 18.: Response of sensors on RMSB versus time – readout every 10 minutes. Left: high sensitivity pin diode. Black (wiggly) line shows raw measurements. After temperature correction (red line) the RMS of measurements is 0.5 mV. From this and the slope in Fig. 9 we estimate that the system is sensitive to 1 MeV equivalent neutron fluences of about 10^8 n/cm^2. Right: High sensitivity RADFET. RADFET was exposed to radiation from [22]Na source for about 80 hours. The increase of voltage due to irradiation can clearly be seen and the sensitivity is better than 1.5 mGy.

5   Summary

Up to now we tried to give a biref overview of the ATLAS radiation monitoring system. Selected radiation sensors, radiation monitor board and readout system were presented. In the rest of the document design details, drawings and photos are collected.

Appendix – Design details, drawings, photos etc….

5.1   Inner Detector radiation monitors

5.1.1   Locations of radiation monitors

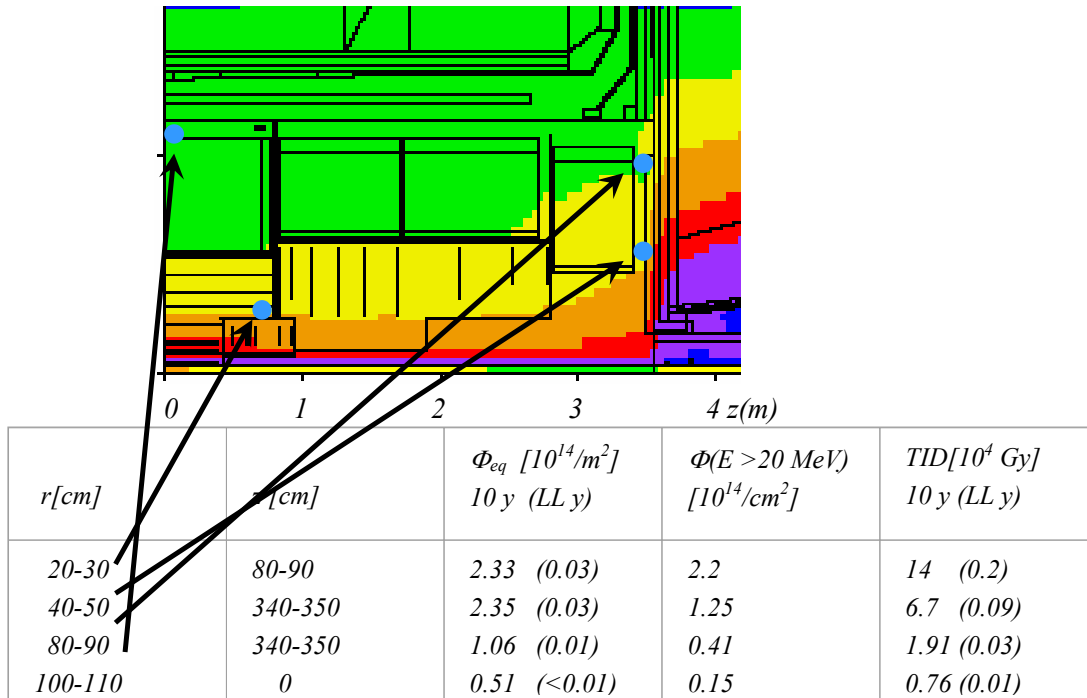| r[cm]	z[cm]	Φ_{eq} [$10^{14}/m^2$] 10 y (LL y)	$\Phi(E >20\ MeV)$ [$10^{14}/cm^2$]	TID[10^4 Gy] 10 y (LL y)
20-30	80-90	2.33 (0.03)	2.2	14 (0.2)
40-50	340-350	2.35 (0.03)	1.25	6.7 (0.09)
80-90	340-350	1.06 (0.01)	0.41	1.91 (0.03)
100-110	0	0.51 (<0.01)	0.15	0.76 (0.01)

Fig. 20: The table contains approximate r and z coordinates of locations of radiation monitors at φ = 0° and expected radiation doses at these locations.

There will be 14 radiation monitors in the inner detector. Monitors at locations with z ≠ 0 will be at: on side A at φ = 0° and at φ = 180°, on side C at φ = 90° and at φ = 270°. There will be 2 monitors at z = 0, one at φ = 0° and the other at φ = 180°.

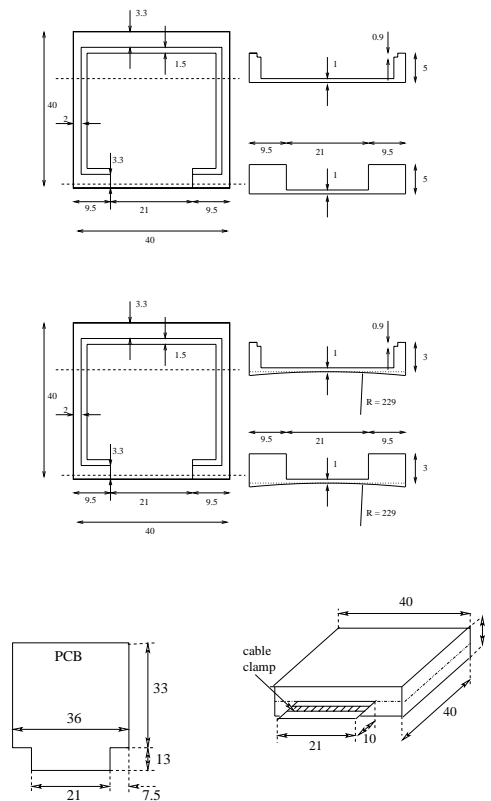### 5.1.2   Housing of Inner Detector RMSBs (ID-RMSB)

Fig. 21: The drawing of the IDMSB using. It is made of two parts – top and bottom - with the RMSB hybrid and PCB frame sandwiched between. Bottom parts of housings which will be glued to Pixel Support Tube is milled to the tube radius (229 mm). Others are made flat. Twisted pairs are soldered to the PCB and fixed with a clamp as can better be seen in the photo in the text (Fig 16). The two parts are fixed together with three M2 nylon screws.

5.1.3 Connections of the ID-RMSB

The ID-RMSBs will be connected to ELMB by a SCT module TYPE II cable (PP2-PP1, max length 16 m) and copper-clad aluminium twisted pairs in a heat shrink from PP1 to RMSB where it will be soldered to the hybrid. There will be a PCB at PP1 with FCI connectors to connect twisted pairs with Type II cable. Drawing of PP1 board is shown in the figure below.
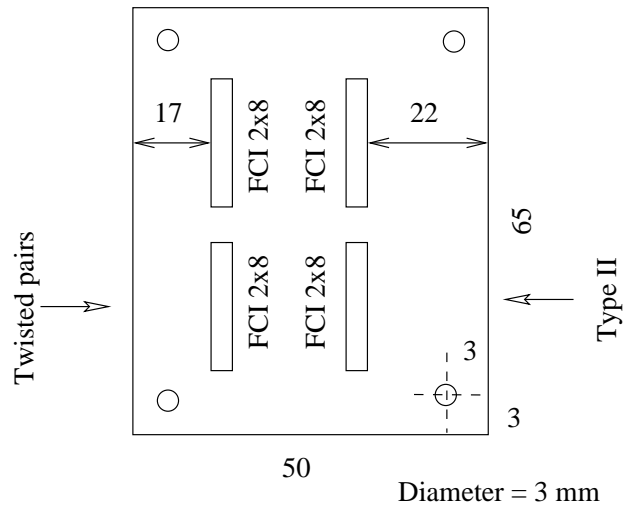
Figure 22: Connections of twisted pairs to TYPE-II cable at Patch Panel 1.

5.1.4   Patch panel board

At PP2 Type-II cable will be connected with FCI 2x8 pin connector to the patch panel board. This board connects sensors to DAC and ADC channels. It hosts the circuitry for voltage attenuators, to adapt the voltages on sensors to the range of ADCs, circuitry needed for ESD protection and read-out of DMILL transistors, circuit for temperature measurement and circuit for the switch (basically a JFET transistor, which will be opened by applying voltage from DAC to it before starting the readout procedure) which will short the pins of the RadFETs and PIN diodes during irradiation and open them during readout. Scheme of the patch panel board is shown in Fig 20.

Return line will be connected to ground ove a 100 Ohm resistor. The voltage on this resistor will be measured by ADC (IMON line) to monitor the current flowing through the sensor being read out. The small (2.5 or 25 uA, depending on the value of the resistor connected in series with NTC) current which is continuously going through the temperature sensor must be subtracted. As can be seen, 13 DAC channels and 13 ADC channels are needed for one ID-RMSB. To simplify the connections, one DAC board (16 channels) and one ELMB input socket (16 ADC channels) will be connected to each PP2 to serve each ID-RMSB.
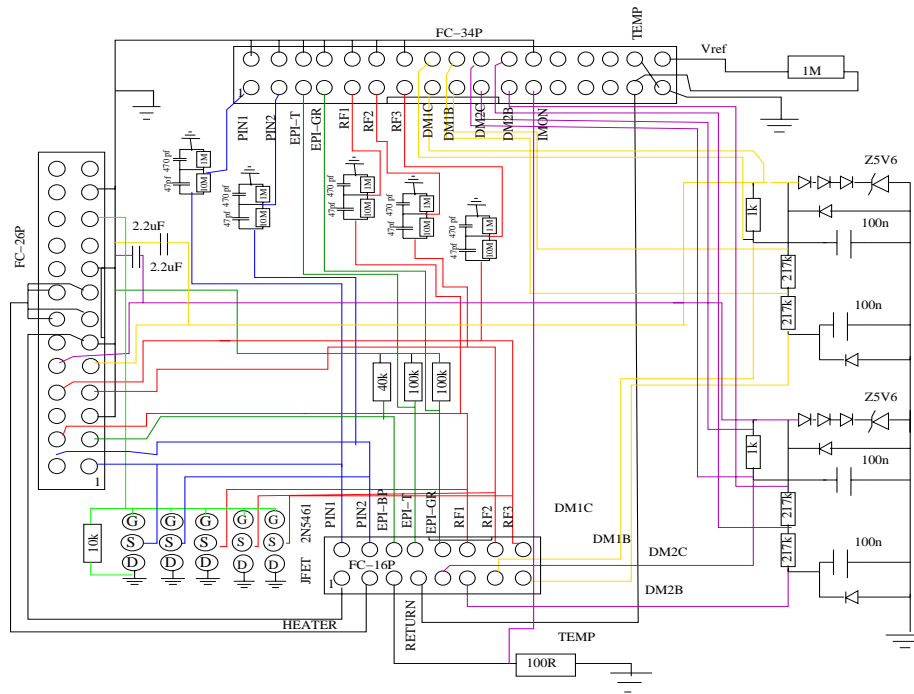
Figure 23: Schematic view of the PP2 Patch panel for the ID-RMSB. Dimension of the board is 6.3cm x 6.8cm.

5.1.5   *Cabling for the ID monitor*

ID-RMSB to PP1: 8 copper-clad Al twisted pairs (16 wires) are soldered to RMSB, crimps are put on the other side and placed into FCI 2x8 connector. The wires are protected by heat shrink tube. The transition to Type II cable: 12 thin wires (R = 0.22 Ohm/m), 4 thick wires (R = 0.033 Ohm/m), is done on PP1 PCB (see Fig .19). Type II cable has FCI 2x8 connector crimped on each side and runs from PP1 to corresponding box at PP2. The PP2 box will contain patch-panel boards, DAC boards and ELMB boards. CAN-bus cables and DAC power supply cables will run from the PP2 box to US15 or USA15.

List of cables, locations of PP1 boards, PP2 boxes and US15 racks can be found in EDMS document:

ATL-IC-EP-0013 (ID_global_service_inventory…).

5.1.6   *Ranges of DAC channels for ID monitor*

The range of individual DAC channels is set with value of one resistor per channel on the board [13]. For inner detector radiation monitors we have the following. Default version i.e. as listed in DAC documentation and bill of material, is 20 mA max, output current. Max output is set to 2 mA for channels (counting from 0) 3, 4,5, 6 and 7 (for 3 radfets and 2 DMILLs).

Resistor list: 110 Ohm (20 mA): R14, R16, R20, R42, R44, R48, R49, R56, R58, R62, R63

1.1 kOhm (2 mA): R21, R28, R30, R34, R35

5.1.7   *Cost estimate*

Worst case per inner detector monitoring board:

1. epi-diode   1x 25 CHF = 25 CHF
2. BPW34F PIN diode   2x   5 CHF = 10 CHF
3. CMRP PIN diode   2x 120 CHF = 240 CHF
4. thin oxide radfet   2x 50 CHF = 100 CHF
5. thick oxide radfet 1x 60 CHF = 60 CHF
6. DMILL transistor   2x 25 CHF = 50 CHF
7. NTC   1x 10 CHF = 10 CHF
8. Ceramic hybrid 1x 200 CHF = 200 CHF
9. PEEK housing   1x 100 CHF = 100 CHF
10.ELMB   0.5x 200 CHF = 100 CHF
11.DAC   16x 22 CHF = 352 CHF
12.RMSB-PP2 connect   1x 170 CHF = 170 CHF

TOTAL   1390 CHF

Allowing for some overhead gives price per channel 1.5 kCHF.

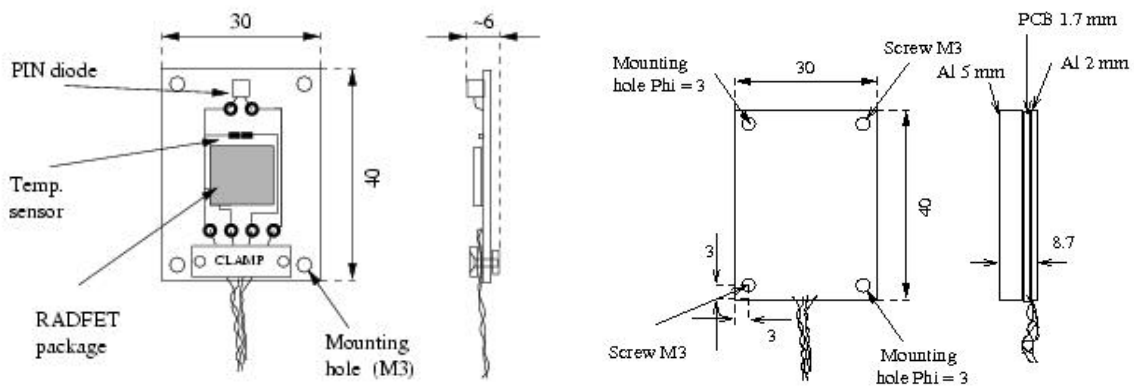## 5.2   Rest of ATLAS radiation monitors

Fig 24: Drawings of ATLAS-RMSB. Left is the scheme of the PCB (compare with the photo in Fig 17). On the right is the RMSB in protection box made of 1 mm thick aluminium. The board is sandwiched between two Al pieces. At the end of the pigtail there is a 4 pin lemo connector of type: FFA.OS.304.CLAK47 (SCEM number 09.31.30.080.0)

5.2.1   Connections of the ATLAS RMSBs

RMSBs outside of the ID need fewer DAC and ADC channels. Each board needs 2 DAC channels (RADFET, diode) and 4 ADC channels (RADFET, diode, temperature, current monitoring).

Since there are 16 channels on each DAC board maximum of 7 RMSBs can be connected to one DAC board because one DAC channel is needed to drive the sensor shorting switch.

In the case of calorimeters RMSBs are connected to a 1.5 m long pigtail (4 wires, twisted pair cable) with 4 pin lemo connector at the end. A cable will connect the RMSB to the patch panel board. In the TILE calorimeter 6 RMSBs will be connected to one patch panel board which will connect 1 DAC board and 2 sockets of ELMB inputs (32 ADC channels). The scheme of the patch panel board circuit is shown in Fig 23.

Fig 22 shows how the RMSBs are connected readout electronics. The cable between RMSB and patch panel can be long – successfully tested with 200 m long cables. The three boards: ELMB, DAC and patch panel must be put close together. ELMB power supply will be used also for DAC power (max 15 volts, but depends on the load on the cable). If possible, additional cable for external power supply will be used to get higher voltage.
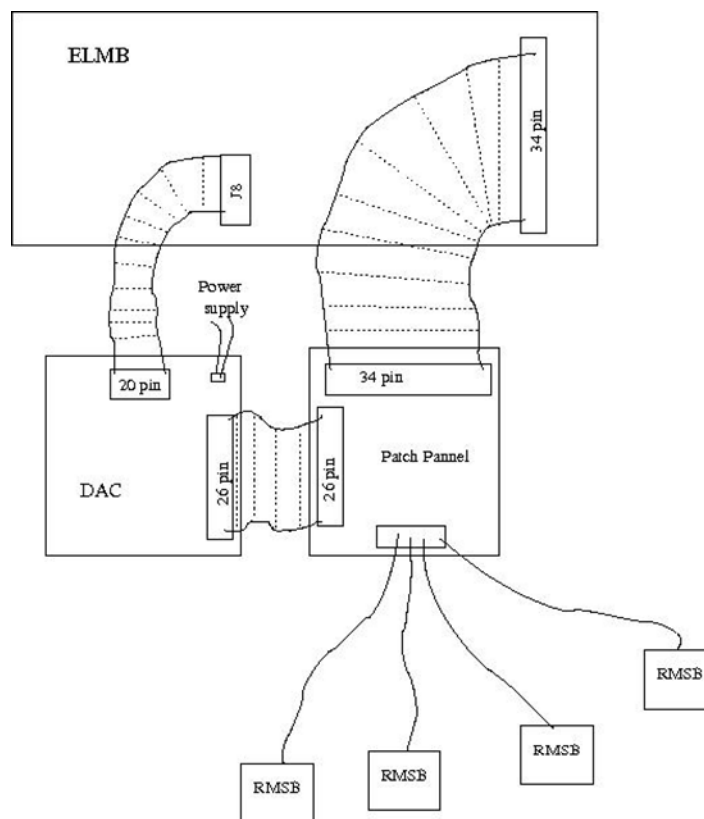

Fig 25: Scheme of connections of RMSBs to patch panel, DAC and ELMB boards
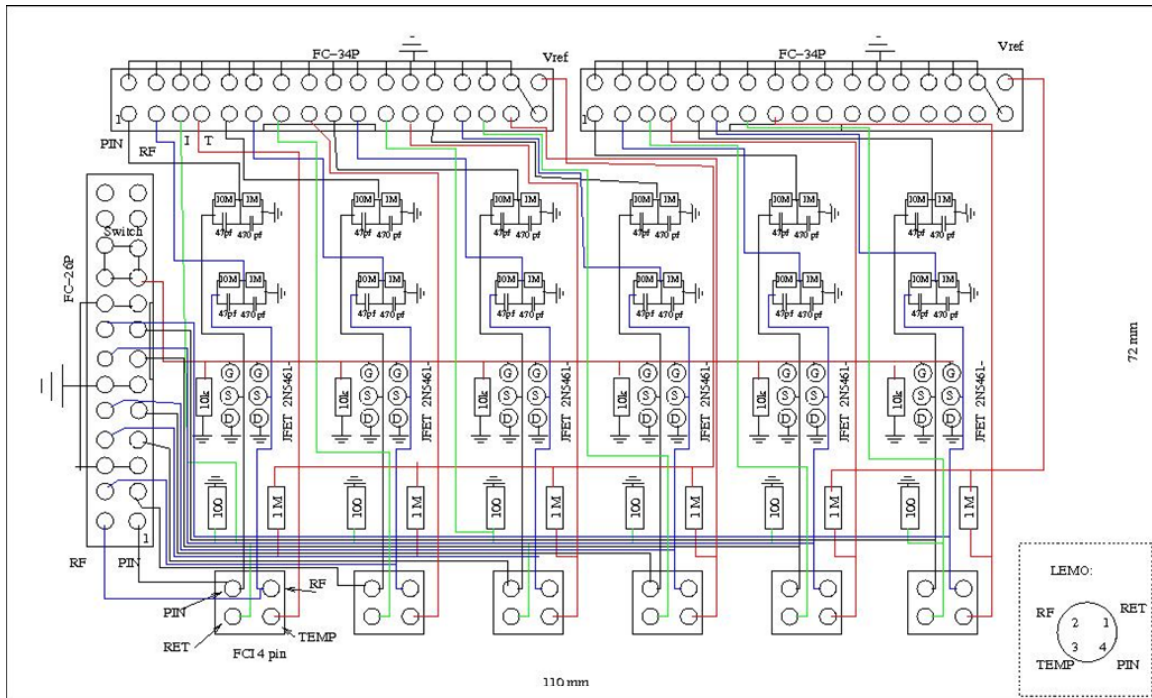
5.2.2 Patch panel board

Fig 26: Scheme of the patch panel board. The definition of connections of pins on LEMO connector (on RMSB pigtail) is shown in the lower right corner. A FCI connector is foreseen for connection of cable to the patch panel board.

5.2.3 Cost estimate

For monitors outside of the ID:

thick oxide radfet :   1x 60 CHF = 60
CMRP PIN diode   :   1x120 CHF = 120
Temperature sensor :   1x 10 CHF = 10
ELMB   :0.25x200 CHF = 50
DAC   :   4x22 CHF = 88
RMSB-ELMB connect :0.25x170 CHF = 43
Housing   :0.25x100 CHF = 25
board   :0.25x200 CHF = 50

TOTAL: 446 C
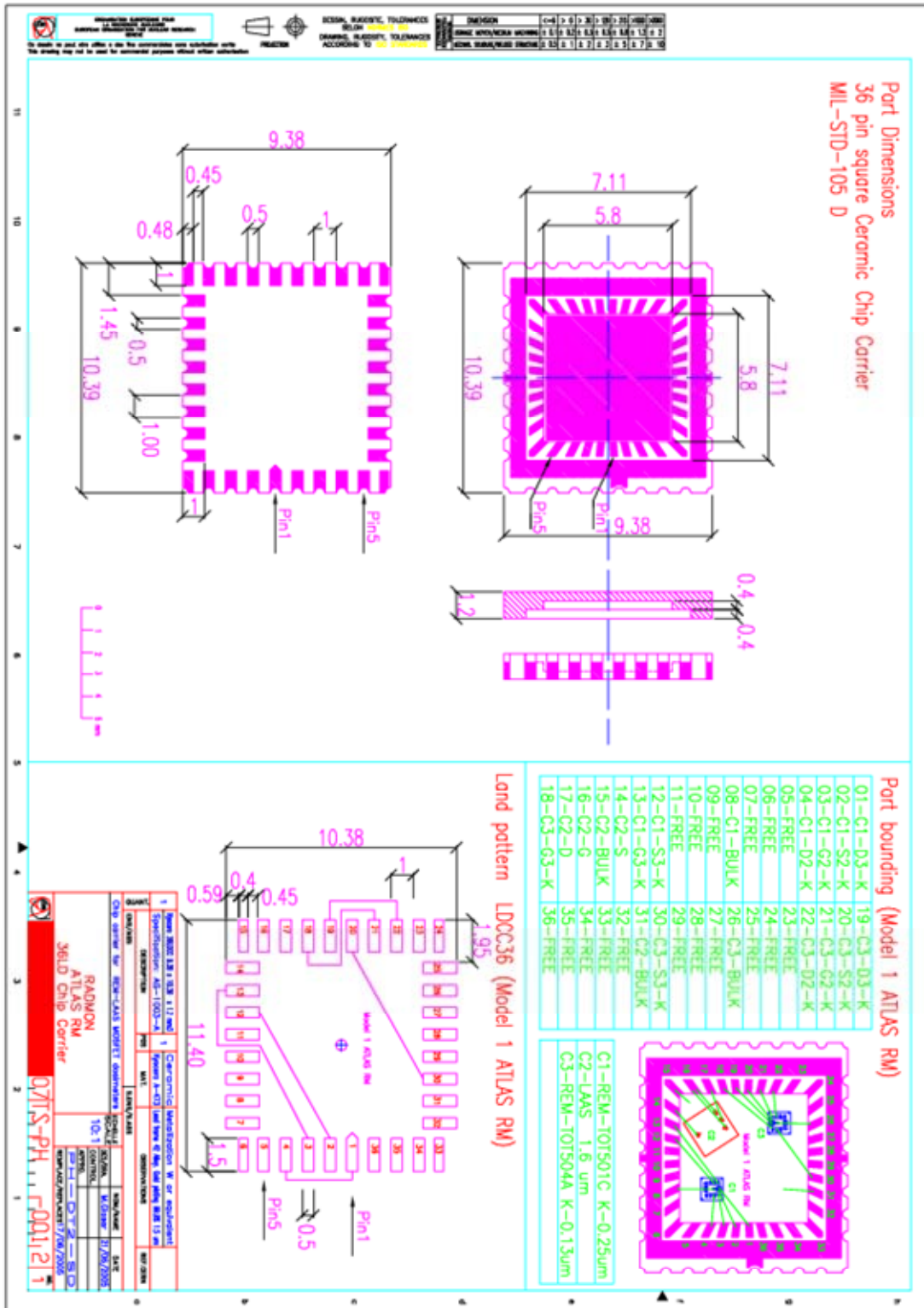
5.3 RADFET packaging and bonding

Fig. 27: RADMON package. For outside of the ID, only one radfet (C2) is mounted into the package.

References

[1] D. Dannheim et. al, "*A Radiation Monitor for the ZEUS Detector at HERA*", IEEE-TNS, Vol. 51, Number 4, 2004.

[2] D. Žontar, "*Radiation monitoring at Belle*", NIM A 501 (2003) 164.

[3] F. Ravotti and M. Glaser, "*Sensor Catalogue*", TS-Note-2005-002, https://edms.cern.ch/file/590497/1/TS-Note-2005-002.pdf

[4] G. Lindström et al.,"*Radiation hard silicon detectors - developments by the RD48 (ROSE) collaboration*", NIM A466 (2001) 308.

[5] G. Kramberger et. al, " *Superior radiation tolerance of thin epitaxial silicon detectors*", NIM A515 (2003) 665.

[6] J. M. Swartz and M. O. Thurston, "*Analysis of the Effect of Fast-Neutron Bombardment on the Current-Voltage Characteristic of a Conductivity-Modulated p-i-n Diode*", J. Appl. Phys., Vol. 37, (1966) pp 744.

[7] M. Tavelt, M.E. Leon-Florian, "*Dose and neutron-fluence measurements in mixed gamma-neutron fileds by means of semiconductor dosimeters*" (IEEE Catalogue RADECS '93, St. Malo, France, 1993, pp. 27-32.

[8] F. Ravotti et al., "*Conception of an Integrated Sensor for the Radiation Monitoring of the CMS Experiment at the Large Hadron Collider*", CERN-PH-EP/2004-04

[9] http://mrp.uow.edu.au/index.shtml

[10] I. Mandić et al., "*Bulk Damage in DMILL npn Biploar Transistors Caused by Thermal Neutrons Versus Protons and Fast Neutrons*", IEEE TNS, Vol. 51, August 2004, pp 1752.

[11] ATI-DC-ELMB-001

[12] ATI-DC-ELMB-002

[13] www.nikhef.nl/pub/departments/ ct/po/html/ELMB/DAC10.pdf